

# COExiST: Revisiting Transmission Count for Cognitive Radio Networks

Guillaume Artero Gallardo  
University of Toulouse - IRIT  
TéSA - Rockwell Collins France  
Toulouse, France  
garterog@alumni.enseeiht.fr

Jean-Gabriel Krieg  
University of Toulouse - IRIT  
Toulouse, France  
jeangabriel.krieg@enseeiht.fr

Gentian Jakllari  
University of Toulouse - IRIT  
TéSA, Toulouse, France  
jakllari@enseeiht.fr

Lucile Canourgues  
Rockwell Collins France  
Blagnac, France  
lucile.canourgues@rockwellcollins.com

André-Luc Beylot  
University of Toulouse - IRIT  
TéSA, Toulouse, France  
beylot@enseeiht.fr

## ABSTRACT

Transmission count, the number of transmissions required for delivering a data packet over a link, is part of almost all state-of-the-art routing metrics for wireless networks. In traditional networks, peer-to-peer interference and channel errors are what define its value for the most part. In cognitive radio networks, however, there is a third culprit that can impact the transmission count: primary user interference. It may be tempting to think of primary user interference as no different than interference caused by other peers. However, unlike peers, primary users do not follow the same protocol and have strict channel access priority over the secondary users. Motivated by this observation, we carry out an empirical study on a USRP testbed for analyzing the impact of primary users. Our measurements show that a primary user has a distinct impact on the transmission count, which the de facto standard approach, ETX, designed for traditional networks, fails to capture. To resolve this, we present CO-ExiST (for COgnitive radio EXpected transMISSion count): a link metric that accurately captures the expected transmission count over a wireless link subject to primary user interference. Extensive experiments on a five-node USRP testbed demonstrate that COExiST accurately captures the actual transmission count in the presence of primary users – the 80th percentile of the error is less than 20%.

## 1. INTRODUCTION

Estimating transmission count – the number of transmissions required for delivering a packet over a link – as a mean to identifying the best links in wireless networks was pioneered by De Couto et al. [8]. Their approach, ETX, has been modified (mostly augmented) many times to include other features, e.g. the physical bit-rate [10]. Its effectiveness and ease of implementation – the broadcast probes remain the most effective and practical solution for a measurement-based link quality estimation – have made it a building block for most modern routing protocols. It has been applied to contexts far beyond the original, including the sensor networks [12], backpressure routing [18], opportunistic routing [11, 16], network coding [14], etc. Nevertheless, despite the diversity of the contexts in which ETX has been applied so far, one thing has always been the same: the link quality has been mostly a function of channel errors and

peer-to-peer<sup>1</sup> interference.

In cognitive radio networks there is a third culprit that can impact the link quality, as perceived by the secondary users: the primary user primacy. Sensing the spectrum [4, 15] to avoid causing harm to primary users is an essential requirement for secondary users, leading to two potential scenarios of throughput loss. One, the spectrum sensing accurately predicts the primary user activity. In this case, secondary users will defer from transmitting, leading to throughput loss<sup>2</sup>. However, the broadcast probes can be queued and released as soon as the primary user ceases transmitting. If the primary user activity lasts less than the size of the moving window ETX uses to estimate loss, say for half of it, all the broadcast probes may end up being delivered by the time the next estimation is performed, making the ETX value of the link perfect. Clearly, this is wrong as only half the channel capacity is available. Ideally, a link metric should penalize this link the same way it does a PU free link where, because of channel errors, two transmissions are required to deliver a data packet. The second scenario of throughput loss occurs when the sensing fails to predict the PU activity. It may be tempting to think of primary user interference in this case as no different than interference caused by other peers. However, there are reasons to believe this may not be the case. For example, with 802.11, a packet transmission is followed by a back-off, which can limit the damage a particular hidden peer interferer can cause, as well as shape how the pattern of losses is perceived by the secondary transmitter. Obviously, primary users do not necessarily use 802.11.

Motivated by these observations, we carry out an empirical study on a five-node USRP testbed network. Our measurements show that when the interferer is a peer node, ETX is pretty adept at approximating the actual transmission count on a particular link. However, keeping everything the same and simply replacing the peer interferer with a primary user leads to significant gaps between ETX and the actual transmission count. Clearly, the primary user is having an adverse

<sup>1</sup>We use the terms peer and secondary user interchangeably.

<sup>2</sup>Channel switching can alleviate the effect of PU interference. However, it does not come free – secondary nodes will have to switch to a new frequency, if one is available, and reconstitute the networks, a process that takes time and coordination. Thus, in many cases simply deferring and waiting the PU out can be a better strategy.

and distinct effect on the capability of two secondary nodes to communicate, which the traditional way of estimating transmission count fails to capture.

We present COExiST<sup>3</sup>, an approach for estimating transmission count over wireless links subject to primary user interference. Its design is driven by our empirical study where we have identified the parameters that best capture the impact of primary user interference on link throughput. In short, COExiST also quantifies the loss of throughput when secondary users are deferring to primary users by calculating the transmission count as if a secondary user transmits instead of deferring and the transmissions result in failure. COExiST can be used as a stand-alone metric for identifying good links or optimal paths in terms of transmission count, or be combined with other parameters, such as the physical bit-rate, for optimizing other performance metrics.

Throughout this paper we make the following contributions:

- In Section 2, we use an USRP N210 testbed to carry out an empirical study on the primary user impact on transmission count. Our data shows that primary users have indeed a distinct effect – something ETX, the de facto standard approach for computing transmission count, fails to capture.
- In Section 3, we use the lessons learnt from the empirical study to design COExiST, an approach for estimating transmission count in cognitive radio networks. Despite the involved computation, COExiST is shown to have a simple, closed-form expression. Furthermore, we show that COExiST coupled with hop-by-hop Dijkstra-based routing satisfies the optimality, consistency and loop-freeness property.
- In Section 4, we describe the development of our prototype testbed using the USRP N210 radio platform and IRIS [21]. We describe our own CSMA/CA implementation and an implementation of COExiST for OLSR.
- In Section 5, we evaluate the performance of COExiST on our USRP testbed. We show that COExiST is very accurate in estimating the transmission count over links subject to primary user interference – 80% of the time the error compared to the actual transmission count is less than 20%. Furthermore, we show that when using COExiST, OLSR selects higher throughput paths than when using ETX as well as two metrics proposed for cognitive radio networks [19, 23].

## 2. PRIMARY USER IMPACT ON TRANSMISSION COUNT

We present an empirical study on the impact of primary user interference on transmission count. Our measurements show that primary users present a distinct challenge when it comes to estimating the transmission count – something ETX, the de facto standard approach of estimating transmission count, fails to capture. We explore the reasons why and provide pointers to potential solutions.

### 2.1 Experimental Setup

**Hardware:** Our testbed consists of five USRP N210 [3] software defined radios coupled with SBX daughterboards

<sup>3</sup>Cognitive radio EXpected transmiSSion count.



**Figure 1:** All our experiments are carried out on a five-node USRP N210 testbed.

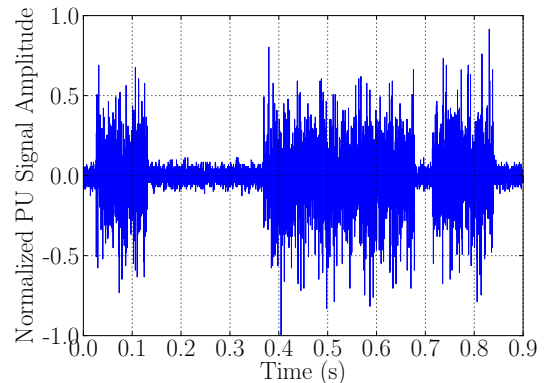


**Figure 2:** A 1-second sampling of the primary user activity, as utilized in our experiments.

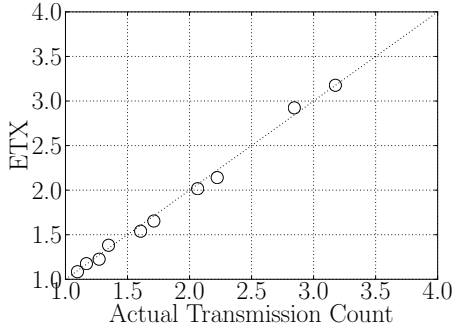
providing a 400-4400MHz frequency range. The SBX daughterboard is equipped with two front-ends: one TX/RX used for secondary user communications, and one RX2 dedicated to spectrum sensing. Each USRP is connected to 64-bit host computers running the Ubuntu 12.04 LTS system (Fig. 1).

**Software:** We use IRIS [21], an open source LGPLv3 software defined radio architecture. Unlike the GNURadio, IRIS is designed specifically to support maximum reconfigurability while the radio is running, a capability that better fits our needs for a cognitive radio testbed. IRIS does not come with a MAC protocol implementation so we augmented its architecture to allow for carrier sensing and implemented the DCF part of the 802.11 MAC. At the routing layer we use OLSR with an ETX implementation. The complete details of the software architecture can be found in Section 4.

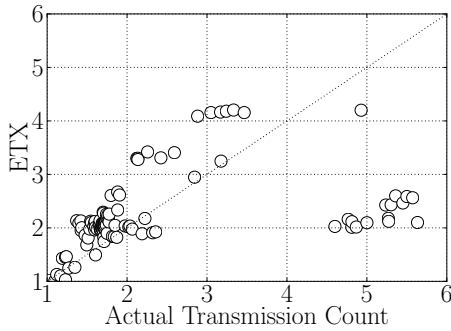
**Emulating Primary Users:** We model the primary user activity by transmitting packets using a high power level, thus interfering with SU communications. To shape the ON/OFF periods we vary the burst duration according to typical continuous time distributions such as the exponential or uniform [15]. Figure 2 shows a typical primary user behavior as utilized in our experiments.

### 2.2 Impact of Primary Users on Transmission Count

To study the potential impact of primary users, we set up a simple 2-node link – a third node acts as interferer



(a) **Interferer is a Peer.** There is a data point for every value of channel reliability considered.

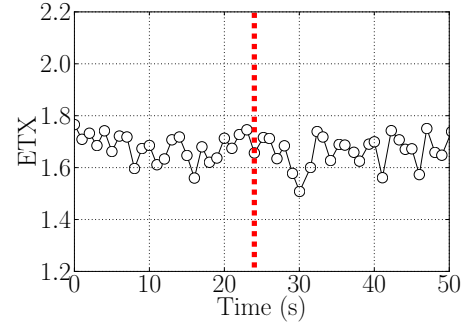


(b) **Interferer is a Primary User.** There is a data point for every combination of channel reliability and primary user activity.

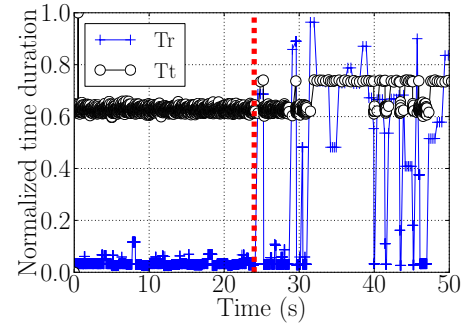
**Figure 3: Primary Users Present a Distinct Challenge when Estimating Transmission Count: The de facto standard approach, ETX, captures well the transmission count when the interferer is a peer (a) but fails to do so when we replace the peer interferer with a primary user (b).**

and switches roles between being a peer and a primary user. UDP packets are sent as fast as possible over the link and we collect the actual transmission count as well as ETX, as reported by the OLSR implementation. We repeat the experiment for a variety of PU levels, 0.2 to 0.7, and link reliabilities (counting only channel attenuation), 0.5 to 1.

Figure 3(a) shows ETX and actual transmission count when the interferer is a peer. Here, the peer is running the same CSMA protocol as the other two nodes and the transmission count is mostly due to channel errors, something ETX estimates fairly well. When we replace the peer interferer with a primary user, things change: Figure 3(b) shows ETX performing poorly. This is due to the fact that ETX estimates the channel quality by sending (broadcast) packets on a regular basis and assumes the transmission failures are independent. However, when failures are due to primary user activity there is a high correlation between them, and the transmission count will highly depend on things like how active the primary users are, the pattern of their activity, etc.



(a) PU becomes active at time 25s and its activity duration is shorter than the moving window ETX uses to estimate loss, leading the latter to completely miss the PU existence.



(b) PU activity starts at time 25s.  $T_t$  and  $T_r$  are averages over 10 samples.

**Figure 4: Capturing Primary User Activity: ETX shows a poor correlation to PU activity. However, the time between two transmissions,  $T_t$ , and the time between two retransmissions,  $T_r$ , show a strong correlation to it.**

### 2.3 Capturing the Impact of Primary Users

Having shown that ETX fails to capture the full impact of primary users on transmission count, we turn our attention to exploring alternative ways that will. Intuition says that, while the probe packets ETX uses may miss a good chunk of the primary user activity, the time a particular node spends to successfully transmit unicast packets could be a good indication of the PU activity.

To verify our intuition, we perform the following experiment. We use the same 3-node topology as before, with two USRP nodes functioning as the secondary network while the third as a primary user. One of the secondary nodes transmits UDP packets to its peer as fast as possible for 50 seconds. The primary node is silent for the first 25 seconds and is activated for the last 25. During the experiment, at the routing layer we collect the ETX values computed by OLSR, while at the MAC layer, the time between a successful transmission and the next attempt,  $T_t$ , and the time between two retransmissions,  $T_r$ .

Figure 4 shows the observed values for ETX (Fig. 4(a)) and the normalized values for  $T_t$ ,  $T_r$  (Fig. 4(a)), as function of

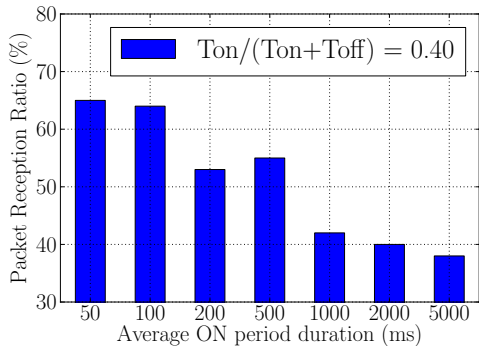


**Figure 5: Not all PU Availabilities are Created Equal: All points represent experiments with the same ratio of PU availability; what changes are the absolute values of ON and OFF. Higher values of ON and OFF lead to lower packet reception ratios, and consequently, higher transmission count.**

the experiment time. The data shows that, while ETX shows a poor correlation to PU activity,  $T_t$  and  $T_r$  show a strong correlation to it. This is due to the fact that the moving window ETX uses to estimate link losses is larger than the average PU ON period, leading to almost all broadcast probes being delivered. On the other hand, the time spent deferring to the primary users is well captured by  $T_t$  and  $T_r$ .

## 2.4 Would a Straightforward Solution Work?

When presented to the challenge of estimating the impact of a primary user on transmission count, the straightforward solution that may cross one’s mind is to treat the primary user as yet another probabilistic source of error, use history to estimate the ratio of time a primary user is active, and simply multiply ETX by this value. Figure 5 shows that this would not work. The data collected using the 3-node topology, with one node acting as a primary user, shows that for the same ratio of PU activity, different values of ON periods have a different impact on the packet delivery ratio.

## 2.5 Summary

The above empirical study shows the following:

- Primary users present a distinct factor impacting the transmission count.
- The traditional way of computing the transmission count, ETX, is well adept at capturing peer interference and channel errors but fails when it comes to Primary User interference.
- The straightforward solution of multiplying ETX by the primary user availability can perform poorly.
- A cross-layer approach using MAC layer information can significantly improve our capability to capture the impact of primary users.

## 3. COEXIST

In this section, we present the design and computation of COExiST. As suggested by the empirical study in Section 2,

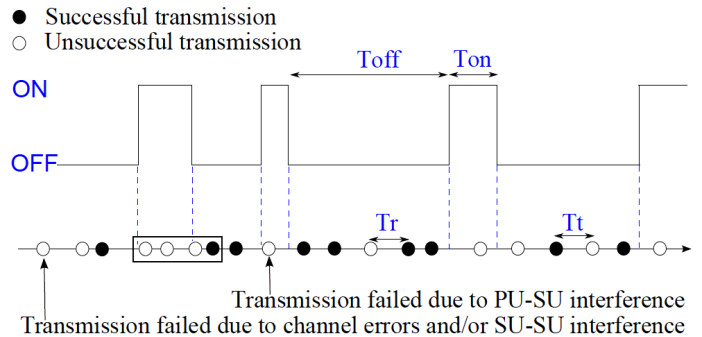


**Figure 6: PU and SU networks operating simultaneously. The primary user activity is modeled as an alternative ON/OFF process.**

to account for the impact of primary users on transmission count, COExiST utilizes the perceived primary user activity, the time between a successful transmission and the next attempt,  $T_t$ , and the time between two retransmissions,  $T_r$ .

## 3.1 Model & Preliminaries

We derive the COExiST of a given link using the network model defined in Figure 6. We use  $u$  to denote the Primary User duty cycle [17] and  $\bar{T}_{on}$ ,  $\bar{T}_{off}$  to denote average primary user ON/OFF period durations, respectively. These quantities are related by the formula  $u = \bar{T}_{on}/(\bar{T}_{on} + \bar{T}_{off})$  [13, 15]. We model the distributions of the primary activity/non-activity periods using exponential distributions with parameters  $\bar{T}_{on}$  and  $\bar{T}_{off}$ . In practice, such period durations are not always exponentially distributed and depend on the primary network characteristics. Nevertheless, as pointed out in [17], the exponential distribution is shown to be a suitable fit for the empirical distributions observed for commercial systems, such as cellular networks. To keep the computation tractable, the same approximation is also used for  $T_r$  and  $T_t$ . COExiST, utilizes the probability of successfully transmitting a packet during the OFF period,  $p_s^{off}$ , to account for the effect of channel errors and SU-SU interference. Finally, similar to ETX [8], our model assumes an unlimited number of transmission attempts at the MAC layer.

## 3.2 Analytical Computation

Let  $N \in \mathbb{N}^*$  be the total number of MAC layer attempts required to successfully transmit a packet over the link. COExiST estimates  $\mathbb{E}[N]$  by resolving an absorbing discrete-time Markov Chain.

**Definition 1.** We model the Cognitive Radio MAC layer retransmission scheme using an absorbing discrete-time Markov chain, with the states defined as follows:

- $I_0$ : The last packet has been successfully transmitted during the OFF state in the Primary channel. The first transmission attempt of the current packet is pending during the OFF state for which the Primary channel is considered Idle. (**initial state**)
- $B_0$ : The last packet has been successfully transmitted during the OFF state in the Primary channel. The first transmission attempt of the current packet is pending during the ON state for which the Primary channel is considered Busy. (**transient state**)

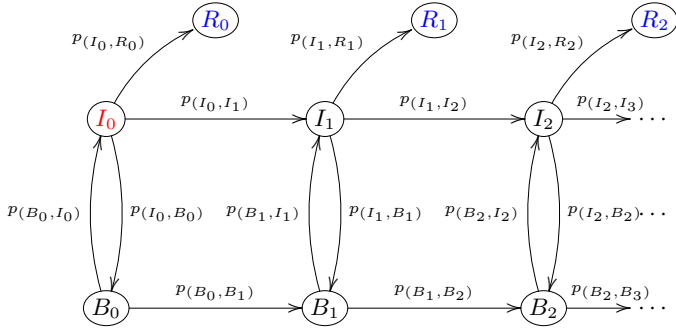


**Figure 7: The absorbing discrete-time Markov chain for computing COExiST.**

- $I_k, k \in \mathbb{N}^*$ : The packet has been transmitted  $k$  times without any success. The retransmission is pending during the OFF period for which the Primary channel is considered Idle. (**transient state**)
- $B_k, k \in \mathbb{N}^*$ : The packet has been transmitted  $k$  times without any success. The retransmission is pending during the ON period for which the Primary channel is considered Busy. (**transient state**)
- $R_k, k \in \mathbb{N}$ : The packet has been successfully transmitted with a total of  $k$  retransmissions (**absorbing state**)

The corresponding Markov Chain, illustrated in Figure 7, has an infinite number of states. It converges probabilistically to one of the absorbing state,  $R_k$ , where  $k$  represents the number of retransmission attempts performed for successfully transmitting a particular packet over the link. The transition probabilities are defined  $\forall k \in \mathbb{N}$  as follows:

- $p_{(I_k, R_k)}$  = Probability that the  $(k+1)^{th}$  transmission attempt is successful **and** takes place before the end of the current OFF period,
- $p_{(I_k, I_{k+1})}$  = Probability that the  $(k+1)^{th}$  transmission attempt is unsuccessful **and** takes place before the end of the current OFF period,
- $p_{(I_k, B_k)}$  = Probability that the  $(k+1)^{th}$  transmission attempt takes place after the end of the current OFF period,
- $p_{(B_k, I_k)}$  = Probability that the  $(k+1)^{th}$  transmission attempt takes place after the end of the current ON period,
- $p_{(B_k, B_{k+1})}$  = Probability that the  $(k+1)^{th}$  transmission attempt takes place before the end of the current ON period.

The above transition probabilities depend on the modeling parameters: the success probability  $p_s^{off}$ , the duty cycle  $u$ , the average ON/OFF period durations  $\bar{T}_{on}$  and  $\bar{T}_{off}$ , as well as the average MAC layer durations  $\bar{T}_r$  and  $\bar{T}_t$ . These transition probabilities, for the most part, do not depend on the rank of the transmission attempt. For the case of  $k = 0$ , they depend on  $\bar{T}_t$  but not  $\bar{T}_r$ . For the case of  $k \neq 0$ , they are identically expressed except that  $\bar{T}_t$  is replaced with  $\bar{T}_r$ . Therefore, the Markov chain is composed of two homogeneous regions. One is composed of the states  $I_0$  and  $B_0$  while the other of all the remaining states. As a result, the Markov chain can be partially solved on both regions for computing COExiST.

**Lemma 1.** The Markov chain transition probabilities satisfy the following relations:

- $p_{(B_k, B_{k+1})} = 1 - p_{(B_k, I_k)}$
- $p_{(I_k, I_{k+1})} = (1 - p_s^{off}) \times (1 - p_{(I_k, B_k)})$
- $p_{(I_k, R_k)} = p_s^{off} \times (1 - p_{(I_k, B_k)})$

Denoting by  $f_{(I_0, R_k)}$  the probabilities of reaching the absorbing state  $R_k, k \in \mathbb{N}$  when starting from the initial state  $I_0$ , the expected transmission count equals

$$\mathbb{E}[N] = \sum_{k=0}^{+\infty} (k+1) f_{(I_0, R_k)} \quad (1)$$

This requires the calculation of the Markov chain transition probabilities as well as the reaching probabilities  $f_{(I_0, R_k)}$ .

1) *Transition probabilities:* Denoting by  $\hat{T}_{on}$  the residual time in the ON period and applying the memoryless property of the exponential distribution, we have  $\hat{T}_{on}$  distributed identically with  $T_{on}$ , that is,  $\hat{T}_{on} \sim \mathcal{Exp}(1/\bar{T}_{on})$ . Exactly the same analysis can be done with  $T_r$ , for which  $\hat{T}_r$  represents the residual time before the next retransmission takes place. With these, the computation of the transition probability  $p_{(B_k, B_{k+1})}$  is as follows:

$$\begin{aligned} p_{(B_k, B_{k+1})} &= \int_{t=0}^{+\infty} \mathbb{P}[\hat{T}_r < t] f_{\hat{T}_{on}}(t) dt \\ &= \int_{t=0}^{+\infty} \mathbb{P}[T_r < t] f_{T_{on}}(t) dt = \frac{1}{1 + \bar{T}_r/\bar{T}_{on}} \end{aligned}$$

Using the relations from Lemma 1 and introducing the variable  $\rho_r$  such that  $\rho_r = \bar{T}_r/(\bar{T}_{on} + \bar{T}_{off})$  we have:

$$p_{(B_k, B_{k+1})} = \frac{u}{u + \rho_r} \quad \text{and} \quad p_{(B_k, I_k)} = \frac{\rho_r}{u + \rho_r}$$

Similarly, for the three remaining transition probabilities:

$$p_{(I_k, B_k)} = \frac{\rho_r}{1 - u + \rho_r} \quad p_{(I_k, R_k)} = \frac{p_s^{off}(1 - u)}{1 - u + \rho_r}$$

$$p_{(I_k, I_{k+1})} = \frac{(1 - p_s^{off})(1 - u)}{1 - u + \rho_r}$$

For the expressions of the transition probabilities involving states  $I_0$  and  $B_0$ ,  $\rho_r$  is replaced with  $\rho_t = \bar{T}_t/(\bar{T}_{on} + \bar{T}_{off})$ .

2) *Reaching probabilities:* Computing the reaching probabilities in an absorbing discrete-time Markov chain can be done by applying the reachability equation, whose definition is repeated below:

**Definition 2** (REACHABILITY EQUATION). The probability of reaching state  $j$  starting from state  $i$  can be computed as:

$$f_{(i, j)} = p_{(i, j)} + \sum_{\forall k \neq j} p_{(i, k)} \times f_{(k, j)} \quad (2)$$

**Theorem 1** (COExiST). The expected transmission count over a link subject to primary user interference is:

$$\mathbb{E}[N] = \frac{1}{p_s^{off}(1 - u)} + \frac{u}{\bar{T}_r} \times \frac{\bar{T}_t - \bar{T}_r}{\bar{T}_t/\bar{T}_{on} + 1 - u} \quad (3)$$

PROOF. Applying the reachability equation on the first region of the Markov chain leads to:

$$f_{(I_0, R_0)} = \frac{P_{(I_0, R_0)}}{1 - P_{(I_0, B_0)}P_{(B_0, I_0)}}$$

and for  $k \in \mathbb{N}^*$ :

$$f_{(I_0, R_k)} = \frac{P_{(I_0, I_1)}f_{(I_1, R_k)} + P_{(I_0, B_0)}P_{(B_0, B_1)}f_{(B_1, R_k)}}{1 - P_{(I_0, B_0)}P_{(B_0, I_0)}}$$

Since:

$$\mathbb{E}[N] = \sum_{k=0}^{+\infty} (k+1)f_{(I_0, R_k)} = \underbrace{\sum_{k=0}^{+\infty} f_{(I_0, R_k)}}_{=1} + \sum_{k=0}^{+\infty} kf_{(I_0, R_k)}$$

the desired result follows from applying Lemma 2.  $\square$

**Lemma 2.** *Computing the analytical expressions of the reaching probabilities leads to the following equations:*

$$\sum_{k=1}^{+\infty} kf_{(I_1, R_k)} = \frac{1}{p_s^{off}(1-u)} \quad (4)$$

$$\sum_{k=1}^{+\infty} kf_{(B_1, R_k)} = \frac{1}{p_s^{off}(1-u)} + \frac{u}{\rho_r} \quad (5)$$

PROOF. Applying recursively the reachability equation, starting from states  $I_1$  and  $B_1$ , and performing some linear combinations on the resulting equations leads to recursive expressions of the desired reaching probabilities, as given for  $k \in \mathbb{N}^*$  by Equations 6 and 7. Therefore, these reaching probabilities satisfy the same linear second-order recurrence equations. However, they differ on their first terms, making the obtained probability values entirely different for the remaining terms of both sequences.

Each linear second-order recurrence equation can be solved for  $k > 1$  using the following well-known method:

1. Compute the roots  $r_1$  and  $r_2$  of the characteristic polynomial  $Q$  given in Equation 8.
2. Compute  $f_{(I_1, R_1)}$  and  $f_{(I_1, R_2)}$  (respectively  $f_{(B_1, R_1)}$  and  $f_{(B_1, R_2)}$  for the second equation)
3. Compute  $\lambda_I$  and  $\mu_I$  (respectively  $\lambda_B$  and  $\mu_B$  for the second equation) such that

$$\begin{cases} \lambda_I + \mu_I & = f_{(I_1, R_1)} \\ \lambda_I r_1 + \mu_I r_2 & = f_{(I_1, R_2)} \end{cases}$$

4. Finally, combine the results:  $f_{(I_1, R_k)} = \lambda_I r_1^{k-1} + \mu_I r_2^{k-1}$

Applying this method is straightforward in principle but it presents challenging calculations due to the dependence of the variables on three different parameters:  $u$ ,  $p_s^{off}$  and  $\rho_r$ . The algebraic expressions for  $r_1$ ,  $r_2$ ,  $\lambda_I$  (respectively  $\lambda_B$ ) and  $\mu_I$  (respectively  $\mu_B$ ) are long and complex. They can be computed, however, with the help of a mathematical tool, such as the open source calculation software *Maxima* [2]. Due to the space constraints, we omit these calculations from the analysis.

After checking the convergence requirements, we get:

$$\begin{aligned} \sum_{k=1}^{+\infty} k \times f_{(I_1, R_k)} &= \lambda_I \sum_{k=1}^{+\infty} k \times r_1^{k-1} + \mu_I \sum_{k=1}^{+\infty} k \times r_2^{k-1} \\ &= \frac{\lambda_I}{(1-r_1)^2} + \frac{\mu_I}{(1-r_2)^2} \end{aligned}$$

which simplifies to  $1/[p_s^{off}(1-u)]$ . Similarly, for the second equation, we get:

$$\sum_{k=1}^{+\infty} k \times f_{(B_1, R_k)} = \frac{\lambda_B}{(1-r_1)^2} + \frac{\mu_B}{(1-r_2)^2}$$

which simplifies to  $1/[p_s^{off}(1-u)] + u/\rho_r$ .  $\square$

**Theorem 2** (COEXiST AS A FUNCTION OF ETX). *When the probing packets used for computing ETX are transmitted independently of the primary users activity pattern, COEXiST can be expressed as the following function of ETX:*

$$\mathbb{E}[N] = ETX + \frac{u}{\bar{T}_r} \times \frac{\bar{T}_t - \bar{T}_r}{\bar{T}_t/\bar{T}_{on} + 1 - u} \quad (9)$$

PROOF. The probing packets can be periodically sent in broadcast mode with a higher priority than unicast packets. As per 802.11, the probing packets are neither acknowledged nor retransmitted in case of errors. If every probing packet used for computing ETX is transmitted independently of the primary users activity pattern, the probability for such a probe to be successfully received is:

$$\begin{aligned} &\overbrace{\mathbb{P}[\text{tx ok} | \text{tx during OFF period}]}^{=p_s^{off}} \overbrace{\mathbb{P}[\text{tx during OFF period}]}^{=1-u \text{ by indep.}} \\ &+ \underbrace{\mathbb{P}[\text{tx ok} | \text{tx during ON period}]}_{=0} \mathbb{P}[\text{tx during ON period}] \end{aligned}$$

which is equivalent to  $PRR = p_s^{off}(1-u)$ . As  $1/PRR = ETX$ , that concludes the proof.  $\square$

The value of Theorem 2 is twofold. It shows that ETX is a special case of COEXiST for  $u = 0$  and/or  $\bar{T}_t = \bar{T}_r$ . And more important, in conjunction with Theorem 3 below, it paves the way for leveraging popular ETX implementations to quickly deploy COEXiST. It is the approach we use in Section 4.

**Theorem 3** (ROUTING WITH COEXiST). *COEXiST coupled with hop-by-hop Dijkstra-based routing satisfies the optimality, consistency and loop-freeness properties.*

PROOF. According to [22], establishing the proof is equivalent to demonstrating that the path weight metric is right-monotonic and right-isotonic. As COEXiST is additive, it suffices to show that the metric is non-negative – this is straightforward from Eq. (1).  $\square$

## 4. IMPLEMENTATION

To evaluate COEXiST, we have used the USRP N210 radio platform and the IRIS<sup>4</sup> software package. We have made <sup>4</sup>IRIS is a component-based application whose architecture and parameters are fully reconfigurable. Such reconfiguration, used for instance for tuning the transmission frequency to another vacant channel, can be performed in real-time, something currently not possible with the GNURadio.

$$f_{(I_1, R_{k+2})} = \left( \frac{P(I_k, I_{k+1}) + P(B_k, B_{k+1})}{1 - P(I_k, B_k)P(B_k, I_k)} \right) f_{(I_1, R_{k+1})} - \left( \frac{P(I_k, I_{k+1})P(B_k, B_{k+1})}{1 - P(I_k, B_k)P(B_k, I_k)} \right) f_{(I_1, R_k)} \quad (6)$$

$$f_{(B_1, R_{k+2})} = \left( \frac{P(I_k, I_{k+1}) + P(B_k, B_{k+1})}{1 - P(I_k, B_k)P(B_k, I_k)} \right) f_{(B_1, R_{k+1})} - \left( \frac{P(I_k, I_{k+1})P(B_k, B_{k+1})}{1 - P(I_k, B_k)P(B_k, I_k)} \right) f_{(B_1, R_k)} \quad (7)$$

$$Q(X) = X^2 - \left( \frac{P(I_k, I_{k+1}) + P(B_k, B_{k+1})}{1 - P(I_k, B_k)P(B_k, I_k)} \right) X + \left( \frac{P(I_k, I_{k+1})P(B_k, B_{k+1})}{1 - P(I_k, B_k)P(B_k, I_k)} \right) \quad (8)$$

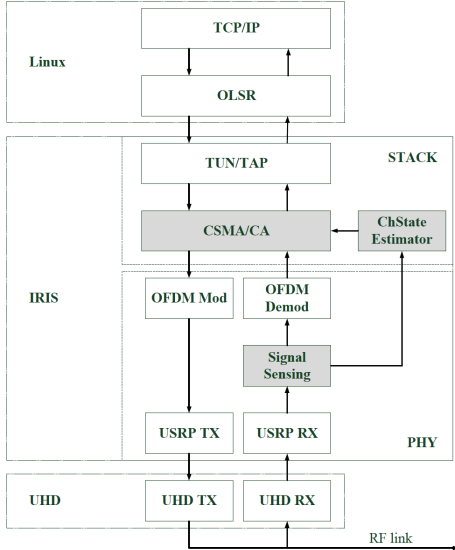


Figure 8: Software Architecture.

significant additions to IRIS that were necessary to run our experiments. Where possible, we used open-source libraries, such as OLSR with ETX, and when not, we added our own implementations, including a CSMA/CA MAC, a primary user model, described in Section 2, and COExiST. Figure 8 shows the architecture of the software running on our testbed.

#### 4.1 CSMA/CA Implementation

IRIS does not yet include a MAC layer component nor any mechanisms that would easily allow running IP applications over USRP radios. To rectify this, we have implemented the DCF (CSMA/CA) part of 802.11.

A main challenge in implementing a CSMA MAC on USRP radios is implementing carrier sensing. We developed our own solution consisting of a *Signal Sensing* component that computes the complex signal recovered by the UHD driver and estimates the power of the received signal or RSSI. The value, coded in 16 bits, is then passed onto the *Channel State Estimator* component at the frequency of once per physical frame received. The *Channel State Estimator* module estimates the current channel state by comparing to a threshold value. For the simple case of a single threshold mechanism, the activity threshold must be calibrated by calculating the noise-floor and adding 10 dB, as recommended by the IEEE 802.11 standard. If the channel state changes, it sends a *Sensing Change* message to the main CSMA/CA component, the equivalent of the Clear Channel Assessment (CCA) in 802.11.

We use the Google protocol buffers to define the structure of the CSMA/CA and leverage the boost library to synchronize the transmission and reception threads inside the main CSMA/CA component. Finally, we interface our MAC layer to the linux IP stack using the Tun/Tap component provided in IRIS.

#### 4.2 COExiST Implementation

We use Eq. 9 from Section 3 to implement COExiST in OLSR. We use OLSRd, an open-source implementation that also includes an implementation of ETX. As Eq. 9 shows, we can leverage the ETX value and add the second term, which is solely a function of  $T_{on}$ ,  $T_r$  and  $T_t$ . Our MAC implementation collects these values and passes them on to OLSR, where a simple modification allows replacing ETX with COExiST. As it does with ETX, OLSR updates COExiST at the default rate of 1/sec. Note that  $T_r$  and  $T_t$  are based on unicast traffic. For bootstrapping the computation and for the cases where there is no unicast traffic, we use the minimum possible values based on the channel access parameters.

### 5. PERFORMANCE EVALUATION

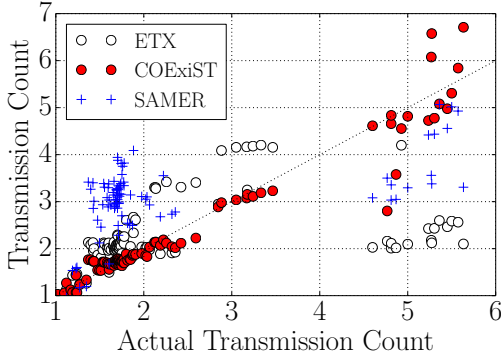
In this section we evaluate the performance of COExiST and compare it with ETX [8], SAMER [19], STOD-RP [23] and the actual transmission count.

In summary, we make the following main observations:

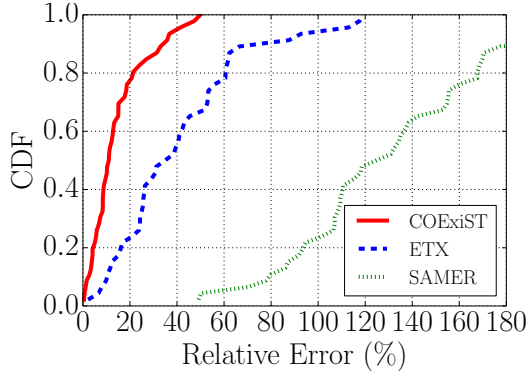
1. In Section 5.2, we show that COExiST is a very good approximation of the actual transmission count – 80% of the time the error is less than 20%. In contrast, the 80th percentile error of ETX is 60% and of SAMER, 160%.
2. In Section 5.3, we show that COExiST continues to provide a very good approximation of the actual transmission count even when the estimation of the primary user activity is erroneous.
3. In Section 5.4, we show that with COExiST, OLSR computes higher throughput paths than with either of the ETX, SAMER or STOD-RP metrics.

#### 5.1 Experimental Setup

Unless otherwise specified, the experimental setup is as follows. The testbed and primary user activity are as described in Section 2.1 while the software architecture as described in Section 4. We carry out two groups of experiments. The first (Sections 5.2 and 5.3) is aimed at evaluating the accuracy of COExiST at estimating the transmission count over a link. For this, three USRP radios are deployed – with two of them representing the secondary network and the third the primary user.



(a) Every data point is an average over three 5-minute experiments.



(b) The CDF of errors for the data from (a).

**Figure 9: Accuracy of COExiST:** For COExiST, 80% of the time the relative error is less than 20%, while for ETX and SAMER is 60% and 160%, respectively.

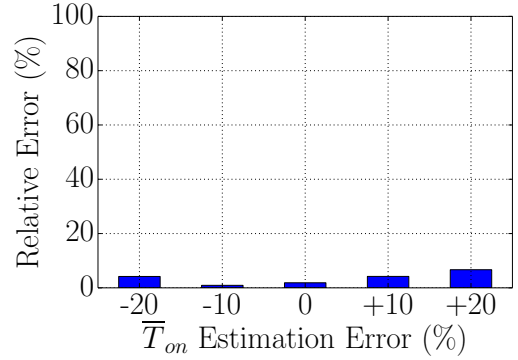
The second group (Sections 5.4) of experiments is aimed at showing the impact COExiST could have on the performance of routing protocols. For this, we use all five USRP radios – with four of them creating a multi-hop secondary network, and the fifth utilized to create up to two primary users. For this group of experiments we connect the USRP radios via RF cables to an RF switch matrix. This enables us to create a multi-hop topology using licensed frequencies and create two primary users using a single USRP.

In all experiments we use Iperf [1] to generate UDP traffic. The radios are configured to send packets at 1Mbps and the data packet size is set to 1500 Bytes. A single experiment runs for 5 mins and the data presented is an average over 3 runs.

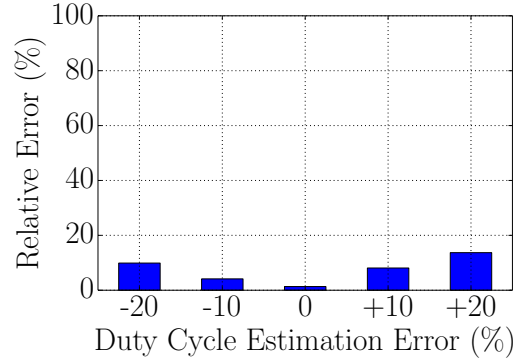
**Basis for Comparison:** We compare COExiST with ETX, the actual transmission count as well as two metrics proposed as part of two routing protocols designed for cognitive radio networks, namely SAMER [19] and STOD-RP [23]. SAMER essentially multiplies the packet reception ratio by the fraction of time with no primary users activity. STOD-RP combines link quality with spectrum availability by dividing ETT [10] by the time duration of the link.

## 5.2 Accuracy of COExiST

To measure the accuracy of COExiST we carry a series of experiments using three nodes, with two nodes represent-



(a)



(b)

**Figure 10: COExiST remains accurate even when it is given erroneous information about the primary user activity.**

ing the secondary network and the third the primary user. Between every experiment we change the placement of all nodes as well as the PU activity pattern. In every experiment we measure the actual transmission count and collect the transmission counts computed by COExiST, ETX and SAMER<sup>5</sup>.

Fig. 9(a) shows that COExiST matches the actual transmission count fairly closely in all the experiments. On the other hand, ETX and SAMER end up either overestimating or underestimating it over a significant number of experiments. More specifically, Fig. 9(b) shows that the 80th percentile error of COExiST is 20%, of ETX is 60% and of SAMER is 160%.

## 5.3 Sensitivity of COExiST to Input Errors

Next, we evaluate the performance of COExiST in the presence of erroneous estimates about the primary user activity. To induce a particular amount of errors, we simply modify the OLSR-COExiST implementation to artificially add errors to the parameters of primary user activity coming from the lower layers. We do this to simulate a real-life scenario where estimation errors are to be expected. Figure 10 shows that despite the significant errors, COExiST maintains

<sup>5</sup>STOD-RP is not included in this experiment as it does not compute the transmission count but rather the transmission time for a successful packet transmission.

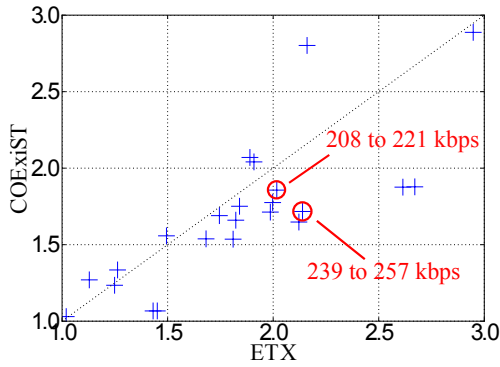


Figure 11: Every data point corresponds to a separate experiment. For two experiments we show the ranges of UDP throughput realized in addition to the respective transmission counts computed by COEXiST and ETX in these experiments. COEXiST is smallest for the point with the higher throughput, while the opposite happens with ETX.

its accuracy.

## 5.4 Transmission Count & Throughput

Finally, we evaluate the impact of an accurate transmission count on throughput. For this we carry out two experiments.

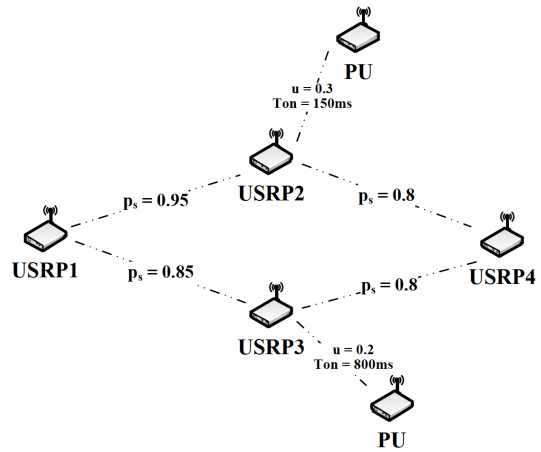
### 5.4.1 Throughput on Single-Hop Paths

In this experiment we use the three node topology and, to overcome the limitation due to the limited number of USRP radios we possess, we try to create in time the equivalent of several links on a multi-hop topology. To do this, we carry multiple experiments where we have a single source transmitting as fast as possible to a single destination while a primary user is interfering and vary the node placement and the PU level of activity from one experiment to another. During each experiment we collect the COEXiST and ETX values as well as the realized UDP throughput. Figure 11 shows the collected values for COEXiST ( $y$ -axis) and ETX ( $x$ -axis) for every experiment. For two experiments we show the respective UDP throughput ranges observed (208 to 221 Kbps for one, 239 to 257 Kbps for the other). ETX is smallest for the experiment where the smaller throughput was realized – 2.0 for 208 to 221 Kbps, 2.2 for 239 to 257 Kbps – while the opposite is observed with COEXiST. The difference observed is obviously due to the time dimension – in a larger network the difference would be due to the space dimension. Either or, a routing protocol minimizing COEXiST would select higher throughput links.

### 5.4.2 Throughput on Multi-Hop Paths

In this experiment, we evaluate the performance of all metrics on the multi-hop topology. In addition to the performance measurements, we also show in Figure 12 the state of the network at the time of the experiment, including the level of channel errors and primary user activity. Note that, as mentioned above, for this experiment, we use an RF switch matrix which allows us to control the channel errors and the level of primary user activity on every link. In the deployed topology, the primary users are hidden to USRP 1.

Figure 12 shows that COEXiST is the only metric that



Path	ETX	SAMER	STOD-RP	COEXiST	Throughput (kbps)
1-2-4	3.51	5.01	0.12	3.48	165.24
1-3-4	3.21	4.01	0.01	3.67	141.12

Figure 12: COEXiST correctly estimates that 1-2-4 is the best path.

identifies the highest throughput path, 1-2-4. This is due to the fact that SAMER considers primary users as a new source of independent channel errors. However, as we have shown in Theorem 2, the packet reception ratio computed by sending broadcast probes is already impacted by the primary user activity. Therefore, multiplying the packet reception ratio by the fraction of time with no primary user activity cannot suffice to capture the actual effect of primary users activity on the transmission count and, ultimately, the realized throughput. On the other hand, STOD-RP adopts a different strategy by considering the absolute time a link is available so as to favor links with less PU activity. However, the absolute time a link is free of PU activity does not tell the whole story – a link can be free of PU activity for a while only with the PU becoming suddenly active. STOD-RP is slow in penalizing such link.

## 6. RELATED WORK

Estimating the transmission count was pioneered by De Couto et al. [8]. It has been modified many times to include other features, e.g., the physical bit-rate [10], and it has been applied to contexts far beyond the original, including to sensor networks [12], backpressure routing [18], opportunistic routing [11, 16], network coding [14], etc.

Nevertheless, ETX was not designed to quantify the impact of primary users on transmission count, as evidenced by its poor performance in our empirical study in Section 2.

In cognitive radio networks, reflecting the unsettled nature of the field, there have been several proposed approaches to routing. Some have advocated for complete system solutions that address joint route-spectrum selection, protection to primary users [9], [7], [20], QoS provisioning [6]. We believe COEXiST is complementary to these approaches. No matter how good the sensing and spectrum assignment are, they cannot guarantee PU free networking. COEXiST can be leveraged for improving routing once the spectrum assignment converges, and it can be used as part of the spectrum assignment decision by quantifying the impact of primary users on performance. Furthermore, combining COEXiST

with traditional routing approaches, as we did with OLSR in this work, can allow for backward compatible solutions that can help the market penetration of cognitive radio networks. Routing metrics for cognitive networks have been proposed in [5, 19, 23]. The works in [19, 23], are built on basically multiplying ETX with a factor characterizing the primary user activity level. However, this approach was shown to perform poorly in our performance evaluation study. OPERA [5] focuses exclusively on delay.

## 7. CONCLUSIONS AND FUTURE WORK

This paper presents COExiST, an approach for estimating transmission count in multi-hop cognitive radio networks. COExiST can be used as a stand-alone metric for quantifying link qualities and computing transmission-count optimal paths, or be combined with other parameters for creating more sophisticated routing metrics, depending on the particular needs. COExiST is measurement-driven, in that, all its inputs are collected at run-time. Using measurements on a five-node USRP N210 testbed, we show that COExiST accurately captures the transmission count for a variety of primary user activity levels and channel errors.

There are several interesting future directions that we are in the process of pursuing. First, it is important to evaluate COExiST on a larger scale testbed and for this we intend to augment the size of our testbed. Second, it will be interesting to explore how COExiST could be used as a building block for creating more sophisticated routing metrics customized for multi-hop cognitive radio networks.

## 8. REFERENCES

- [1] Iperf-tool, <http://dast.nlanr.net/projects/iperf/>.
- [2] Maxima, a computer algebra system. v5.30.0, 2013.
- [3] Ettus Research, A National Instruments Company, <http://www.ettus.com/>, 2015.
- [4] P. Bahl, R. Chandra, T. Moscibroda, R. Murty, and M. Welsh. White space networking with wi-fi like connectivity. In *ACM SIGCOMM*, pages 27–38, 2009.
- [5] M. Caleffi, I. F. Akyildiz, and L. Paura. OPERA: Optimal Routing Metric for Cognitive Radio Ad Hoc Networks. *IEEE Transactions on Wireless Communications*, 11(8):2884–2894, 2012.
- [6] K. R. Chowdhury and I. Akyildiz. CRP: A Routing Protocol for Cognitive Radio Ad Hoc Networks. *IEEE Journal on Selected Areas in Communications*, 29(4):794–804, april 2011.
- [7] K. R. Chowdhury and M. D. Felice. Search: A routing protocol for mobile cognitive radio ad-hoc networks. *Computer Communications*, 32(18):1983–1997, 2009.
- [8] D. S. J. De Couto, D. Aguayo, J. C. Bicket, and R. Morris. A high-throughput path metric for multi-hop wireless routing. In *ACM MOBICOM*, pages 134–146, 2003.
- [9] L. Ding, T. Melodia, S. N. Batalama, and M. J. Medley. Rosa: distributed joint routing and dynamic spectrum allocation in cognitive radio ad hoc networks. In *ACM MSWiM*, pages 13–20, 2009.
- [10] R. Draves, J. Padhye, and B. Zill. Routing in multi-radio, multi-hop wireless mesh networks. In *ACM MOBICOM*, pages 114–128, 2004.
- [11] H. Dubois-Ferrière, M. Grossglauser, and M. Vetterli. Valuable detours: Least-cost anypath routing. *IEEE/ACM Transactions on Networking*, 19(2):333–346, April 2011.
- [12] O. Gnawali, R. Fonseca, K. Jamieson, D. Moss, and P. Levis. Collection tree protocol. In *ACM SenSys*, pages 1–14, 2009.
- [13] C. Jiang, Y. Chen, K. J. R. Liu, and Y. Ren. Renewal-theoretical dynamic spectrum access in cognitive radio network with unknown primary behavior. *IEEE Journal on Selected Areas in Communications*, 31(3):406–416, 2013.
- [14] S. Katti, H. Rahul, W. Hu, D. Katabi, M. Médard, and J. Crowcroft. Xors in the air: practical wireless network coding. *IEEE/ACM Transactions on Networking*, 16(3):497–510, 2008.
- [15] H. Kim and K. G. Shin. Efficient Discovery of Spectrum Opportunities with MAC-Layer Sensing in Cognitive Radio Networks. *IEEE Transactions on Mobile Computing*, 7(5):533–545, May 2008.
- [16] R. P. Laufer, H. Dubois-Ferrière, and L. Kleinrock. Polynomial-time algorithms for multirate anypath routing in wireless multihop networks. *IEEE/ACM Transactions on Networking*, 20(3):742–755, 2012.
- [17] M. López-Benítez and F. Casadevall. Time-Dimension Models of Spectrum Usage for the Analysis, Design, and Simulation of Cognitive Radio Networks. *IEEE Transactions on Vehicular Technology*, 62(5):2091–2104, 2013.
- [18] S. Moeller, A. Sridharan, B. Krishnamachari, and O. Gnawali. Routing without routes: the backpressure collection protocol. In *ACM/IEEE IPSN*, pages 279–290, 2010.
- [19] I. Pefkianakis, S. H. Y. Wong, and S. Lu. SAMER: Spectrum Aware Mesh Routing in Cognitive Radio Networks. *IEEE DySPAN*, pages 1–5, 2008.
- [20] A. Sampath, L. Yang, L. Cao, H. Zheng, and B. Y. Zhao. High Throughput Spectrum-aware Routing for Cognitive Radio Networks. In *CROWNCOM*, 2007.
- [21] P. D. Sutton, J. Lotze, H. Lahlou, S. A. Fahmy, K. E. Nolan, B. Özgül, T. W. Rondeau, J. Noguera, and L. Doyle. Iris: an architecture for cognitive radio networking testbeds. *IEEE Communications Magazine*, 48(9):114–122, 2010.
- [22] Y. Yang and J. Wang. Design Guidelines for Routing Metrics in Multihop Wireless Networks. In *IEEE INFOCOM*, pages 1615–1623, 2008.
- [23] G.-M. Zhu, I. F. Akyildiz, and G.-S. Kuo. STOD-RP: A Spectrum-Tree Based On-Demand Routing Protocol for Multi-Hop Cognitive Radio Networks. In *IEEE GLOBECOM*, pages 3086–3090, 2008.